Current Research in Chemical Biology 1 (2021) 100012

Contents lists available at ScienceDirect

Current Research in Chemical Biology

journal homepage: www.journals.elsevier.com/current-research-in-chemical-biology

XNA enzymes by evolution and design

Turnee N. Malik [a], John C. Chaput [a,b,c,d,*]

[a] Department of Pharmaceutical Sciences, University of California, Irvine, CA 92697-3958, USA
[b] Department of Chemistry, University of California, Irvine, CA 92697-3958, USA
[c] Department of Molecular Biology and Biochemistry, University of California, Irvine, CA 92697-3958, USA
[d] Department of Chemical and Biomolecular Engineering, University of California, Irvine, CA 92697-3958, USA

ARTICLE INFO

Keywords:
Xeno-nucleic acids (XNAs)
Xenobiotic nucleic acids
TNA
FANA
XNAzyme

ABSTRACT

The last decade has witnessed tremendous growth in the field of synthetic genetics, an area of synthetic biology that applies concepts that are commonly associated with the field of genetics, such as heredity and evolution, to artificial genetic polymers with novel backbone structures (XNAs). In addition to the emergence of biologically stable affinity reagents (aptamers), progress in this area has led to the discovery of XNA enzymes (XNAzymes) that are capable of mediating transphosphorylation chemistry with multiple turnover activity. This review explores the evolution and rational design of XNAzymes as well as their potential as reagents in biomedical applications.

1. Introduction

Nature uses a diverse array of enzymes to catalyze all of the chemical reactions required to support cellular function. Although most enzymes are proteins, a subset, called ribozymes, comprise folded RNA structures that are capable of mediating transphosphorylation and peptide biosynthesis reactions. Common examples of naturally occurring ribozymes include the group I and group II self-splicing introns (Cech et al., 1981), RNase P (Guerrier-Takada et al., 1983), the hammerhead and HDV ribozymes (Prody et al., 1986; Wu et al., 1989), and the catalytic core of the ribosome (Nissen et al., 2000). Both protein and RNA enzymes are defined by the primary sequence of their monomeric units, which dictates their ability to fold into secondary and tertiary structures with active sites capable of substrate recognition and catalysis.

The list of chemical reactions catalyzed by ribozymes and related 2′-deoxyribozymes (DNAzymes) has grown considerably due to in vitro selection—a process that applies the principles of Darwinian evolution to large populations of sequences as a way to discover individual molecules with specific functional properties (Joyce, 2004; Silverman, 2008). In vitro selection experiments have produced a panoply of nucleic acid enzymes that catalyze a variety of chemical transformations, including phosphodiester bond cleavage and ligation (Breaker and Joyce, 1994; Ekland et al., 1995), glycosidic and peptide bond formation (Unrau and Bartel, 1998; Zhang and Cech, 1997), ribonucleotide polymerization (Ekland and Bartel, 1996), as well as alkylation (Wilson and Szostak, 1995), acylation (Lohse and Szostak, 1996), and C–C bond formation chemistry (Tarasow et al., 1997). Some of the more notable examples include: (1) flexizymes, flexible tRNA acylating ribozymes capable of using a wide range of amino acid substrates in genetic reprogramming (Goto et al., 2011); (2) DNAzyme 10–23, a therapeutic candidate for gene silencing by site-specific RNA cleavage of disease-associated mRNAs (Santoro and Joyce, 1997; Cho et al., 2013); and (3) the polymerase ribozyme 24-3, which is capable of RNA amplification via a ribozyme-driven polymerase chain reaction (PCR) (Tjhung et al., 2020). Such discoveries provide new insights into pathways that may have led to the emergence of the RNA world and permit a comparison of the functional properties of nucleic acid and protein enzymes.

Progress in understanding the evolution and behaviors of catalytic RNA and DNA molecules has lent itself to the establishment of in vitro selection systems that extend the concepts of heredity and evolution to artificial genetic polymers with novel backbone architectures. Such molecules, commonly referred to as xeno nucleic acids (XNAs), differ from their natural counterparts by the identity of the sugar or sugar-like moiety in their backbone structure (Fig. 1). Thus, just as the 'R' in RNA denotes ribose, the 'X' in XNA refers to the specific sugar unit found in each of the various genetic systems (Chaput and Herdewijn, 2019). For example, ANA refers to the artificial genetic system, arabinose nucleic acid. Although many XNAs have been chemically prepared by solid-phase synthesis, only a subset is capable of Darwinian evolution because in vitro evolution requires engineered polymerases to faithfully copy genetic information back and forth between DNA and XNA, which necessitates that polymerases and reverse transcriptases be evolved to

* Corresponding author. Department of Pharmaceutical Sciences, University of California, Irvine, CA 92697-3958, USA.
E-mail address: jchaput@uci.edu (J.C. Chaput).

https://doi.org/10.1016/j.crchbi.2021.100012

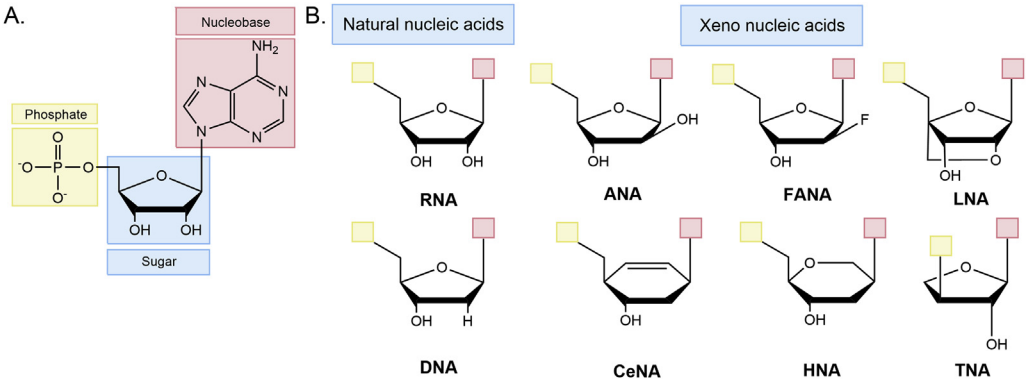

Fig. 1. Sugar moieties of nucleic acids. (A) The generic structure of nucleic acids is shown with the phosphate group highlighted in yellow, sugar group in blue, and nucleobase in pink. (B) Chemical structures of the sugar moieties in natural and select xeno nucleic acids are presented. RNA Color scheme is the same as presented in (A). RNA = ribonucleic acid; DNA = 2′-deoxyribonucleic acid; ANA = arabinose nucleic acid; FANA = 2′-fluoroarabino nucleic acid; LNA = locked nucleic acid; CeNA = cyclohexene nucleic acid; HNA = hexitol nucleic acid; TNA = threose nucleic acid.

recognize XNA triphosphates and XNA templates, respectively, prior to use in XNA selection experiments. While this review focuses on nucleic acid enzymes made from sugar-modified nucleic acids, readers interested in XNA polymerase evolution (Nikoomanzar et al., 2020) or other types of chemically modified nucleic acid enzymes—such as those with nucleobase modifications (Brudno and Liu, 2009; Hollenstein, 2019)—are directed to other articles discussing these topics.

2. Xeno nucleic acids (XNAs)

Relative to natural DNA and RNA, XNAs can have unique physicochemical properties that are often desirable for applications in synthetic biology. Some of the more common attributes include increased biological stability (Culbertson et al., 2016; Kratschmer and Levy, 2017), altered helical geometry (Anosova et al., 2016), and elevated thermal stability (Dunn et al., 2020), all of which are due to the presence of a non-natural sugar in place of the natural ribose or deoxyribose sugars commonly found in RNA and DNA, respectively (Anosova et al., 2016). For example, α-L-threose nucleic acids (TNA) has a four-carbon threose sugar in the backbone structure that is recalcitrant to nucleases that normally recognize ribose and deoxyribose sugars (Culbertson et al., 2016). Likewise, the constrained conformation of locked nucleic acids (LNA) allows for increased thermodynamics of hybridization by 'locking' the ribose sugar into C3′-endo sugar conformation (Kauppinen et al., 2005). In drug discovery, these features could lead to improved pharmacokinetic and pharmacodynamic properties by enabling longer residence times in biological environments or enhanced activity when compared to their natural counterparts. In cellular systems, XNAs offer a route to orthogonal genetic polymers that could provide a genetic firewall between the biological information of the cell and new coding information introduced for synthetic biology applications (Schmidt, 2010; Pinheiro et al., 2013). XNAs are also being evaluated as a biologically stable, soft material for low-energy, high density information storage (Yang et al., 2020). This research, as well as fundamental studies into the origin of our natural genetic system, is laying the groundwork for the broader fields of synthetic genetics and xenobiology.

3. In vitro selection

In vitro evolution enables identification of individual sequences that can perform a desired function from a large population of nucleic acid molecules (Joyce, 2004; Wilson and Szostak, 1999). Genetic polymers are ideally suited for this purpose because they fold into structures with defined functional traits (phenotypes), and their sequences (genotypes) can be replicated by polymerases to produce progeny molecules that share many of the same properties as their parental sequence. The ability to directly amplify genetic sequences with desired phenotypes and optimize their functions by directed evolution distinguishes nucleic acid polymers from other organic molecules, which are generally incapable of replication because they lack a genotype-phenotype connection. One exception is DNA-encoded libraries (DEL), which provide access to small molecule chemistries that maintain a genotype-phenotype connection (Cochrane et al., 2019; Fitzgerald and Paegel, 2021). However, unlike XNAs, DEL libraries do not undergo iterative rounds of selection. Instead, this technique oversamples small molecule repertoires in single, high throughput screening assays to identify small molecule ligands from a combinatorial library of no more than 10^6 members.

Applying the principles of Darwinian evolution to nucleic acids involves subjecting a large population of unique sequences to iterative rounds of selection and amplification. Molecules with a desired functional property are physically separated from the inactive pool, and their genotypes are amplified to generate a new population of enriched molecules with a common functional trait, such as ligand binding or catalysis. Throughout the evolutionary process, the stringency of the selection increases to enrich sequences that function with enhanced activity. For ligand binding selections, this typically involves reducing the concentration of the target or introducing competing targets to guide the pool towards sequences that function with improved binding affinity and specificity. In the case of nucleic acid enzymes, increased stringency is typically achieved by reducing the reaction time and concentration of divalent metal ion used as a cofactor in the reaction. Once the population of evolving molecules converges on a phenotypic trait that cannot be improved without intentional mutagenesis and directed evolution, individual members are identified by DNA sequencing and their activities are characterized using common biochemical methods.

4. Moving beyond DNA and RNA catalysts

Shortly after the first XNA aptamers were discovered by in vitro selection (Pinheiro et al., 2012; Yu et al., 2012), Holliger and colleagues demonstrated that the concepts of heredity and evolution could be extended to synthetic genetic polymers that fold into catalytically active structures (Taylor et al., 2015). XNA catalysts deriving from four different backbone chemistries—arabino nucleic acid (ANA), 2′-fluoroarabino nucleic acid (FANA), hexitol nucleic acid (HNA), and cyclohexene nucleic acid (CeNA)—were isolated with RNA cleavage and ligation activity. Though the ANA, HNA, and CeNA catalysts each displayed slow catalytic rates, a FANA enzyme (FANAzyme) sequence containing a 26-nucleotide catalytic core achieved an observed rate constant (k_{obs}) of 0.06 min^{-1} for magnesium (Mg^{2+})-dependent site-specific RNA cleavage (Fig. 2A). Other FANAzymes discovered in this study catalyzed the ligation of two RNA or FANA substrates, with a k_{obs} of 2×10^{-4} min^{-1} and 0.038 min^{-1}, respectively (Fig. 2B and C).

Although the isolation of XNAs by in vitro selection demonstrated that heredity and evolution are general concepts that can be applied to any type of synthetic genetic polymer, it remained unknown if XNAs

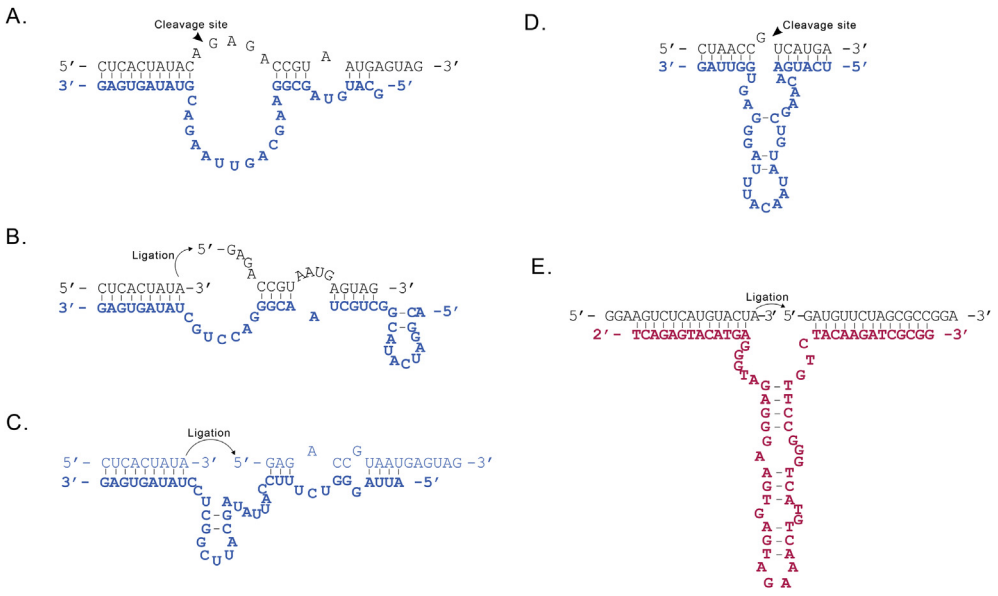

Fig. 2. Examples of XNAzymes. The secondary structures of the (A) FR17_6 RNA endonuclease, (B) F2R17_1min RNA ligase, (C) FpImR4_2 FANA ligase, (D) 12-7 RNA endonuclease, and (E) T8-6 RNA ligase are shown. RNA nucleotides are shown in black, FANA nucleotides in blue, and TNA nucleotides in red. Sequences of enzymes are indicated with bold lettering; all other sequences represent substrates. Arrows indicate sites of cleavage or ligation.

could achieve more efficient catalysis. Efforts to address this question began by establishing a general selection system for evolving FANA molecules that relied on natural (rather than mutant) polymerases to transcribe and reverse transcribe FANA sequences with high efficiency and fidelity (Wang et al., 2018). Chaput and colleagues demonstrated that the replicative DNA polymerase isolated from the thermophilic archaeal species *Thermococcus gorgonarius* (Tgo) mediated efficient FANA synthesis on DNA templates, while a replicative DNA polymerase isolated from the bacterial species *Geobacillus stearothermophilus* (Bst) facilitated efficient DNA synthesis on FANA templates. Using these enzymes, the aggregate fidelity of replication (DNA→FANA→DNA) was determined to be 99.9%, with transcription and reverse transcription rates of ~15 nt/min and ~1 nt/min, respectively. Since these enzymes and FANA substrates are commercially available, this replication platform has made XNA evolution more accessible to laboratories that lack the ability to synthesize specialty XNA triphosphates or express and purify engineered XNA polymerases.

Starting from an unbiased pool of $\sim 10^{14}$ sequences, in vitro selection produced an RNA-cleaving FANAzyme known as FANAzyme 12-7 that functioned with a rate enhancement of $>10^6$-fold over the uncatalyzed reaction and exhibited substrate saturation kinetics typical of most natural enzymes (Wang et al., 2018). The enzyme comprises a small catalytic domain of 25 nucleotides flanked by substrate-binding arms that can be engineered to recognize RNA substrates of diverse sequences (Fig. 2D). The enzyme was found to achieve Michaelis-Menten kinetics with a catalytic activity (k_{cat}) of 0.2 ± 0.01 min^{-1} and a Michaelis constant (K_M) of 600 ± 77 nM. To our knowledge, this was the first report of Michaelis-Menten kinetics for an XNA enzyme. Subsequent evaluation of 12-7 showed that this FANAzyme outperforms a previously evolved DNAzyme at cleaving chimeric DNA substrates that contain a single ribonucleotide at the cleavage site, with $k_{obs} = 0.19$ min^{-1} and $k_{obs} = 0.08$ min^{-1} for FANAzyme 12-7 and the previously described DNAzyme, respectively (Wang et al., 2020). Importantly, these studies not only provided the first evidence that XNAzymes—and particularly, FANAzymes—can rival the capabilities of traditional DNAzymes, but also suggested that XNAzyme production can be optimized to obtain enzymes that possess improved catalytic activity.

The latest example of an in vitro selected XNAzyme is a threose nucleic acid (TNA) enzyme (threozyme) with RNA ligase activity (Wang et al., 2021a). Discovered by Yu and colleagues, the threozyme consists of a 40-nucleotide catalytic core flanked by substrate binding arms complementary to the RNA substrate (Fig. 2E). In the presence of 40 mM Mg^{2+} (pH 9.0), the enzyme catalyzed the formation of a 2′, 5′-phosphodiester bond between the 2′ hydroxyl of the RNA acceptor strand and a 5′ triphosphate of the RNA donor strand with a k_{obs} of 0.01 min^{-1}. As a proof-of-principle demonstration, the threozyme was used to synthesize a functional version of the hammerhead ribozyme by ligating two inactive portions of the RNA sequence together. This study, which is the first report of a threozyme, corroborated previous evidence for TNA as an evolutionary progenitor of RNA (Yu et al., 2012; Kim and Benner, 2017; Colville and Powner, 2021) by providing a possible scenario for the emergence of an RNA world from a simpler genetic material.

5. XNAzymes by design

In addition to in vitro selection, several groups have attempted to improve the activity of known enzyme scaffolds by rational design. A classic example is the RNA-cleaving DNAzyme known as 10–23, which is a highly efficient RNA cleaving motif that has been extensively evaluated in the laboratory and in clinical trials. The 10–23 DNAzyme comprises a 15-nucleotide catalytic core that is flanked on both sides by substrate binding arms that are complementary to the target RNA. Metal-assisted substrate cleavage occurs at a defined purine-pyrimidine dinucleotide junction, with a strong preference for G-U dinucleotides (Santoro and Joyce, 1997). Under optimal reaction conditions, which include elevated Mg^{2+} and pH, 10–23 achieves a catalytic rate of ~10 min^{-1}, and a catalytic efficiency (k_{cat}/K_M) approaching the diffusion-controlled limit (Santoro and Joyce, 1998). However, at lower Mg^{2+} concentrations (2 mM $MgCl_2$, 37 °C, and pH 7.5), the cleavage rate declines to ~0.1 min^{-1} (Santoro and Joyce, 1998), indicating that 10–23 is highly Mg^{2+}-dependent and therefore has limited use in vivo as a gene silencing tool. Nevertheless, the sequence has served as a useful blueprint to guide the design of 10–23 variants that function with enhanced activity or reduced Mg^{2+} dependency. For example, one report showed that modification of select positions in the 10–23 catalytic core with amino acid-bearing nucleotides enables catalysis without Mg^{2+} or other divalent metals (Smuga et al., 2010). A different study revealed that replacement of two thymidines in the substrate binding arms with the

corresponding locked nucleic acids (LNA) results in increased RNA cleavage, likely owing to greater affinity for the substrate by the LNAzyme (Vester et al., 2002). Numerous other studies have also reported the nuclease-protective effects afforded by chemical modifications such as phosphorothioate linkages or inverted 3′ terminal nucleotides (Appaiahgari and Vrati, 2007; Xie et al., 2006).

Chemical optimization of the 10–23 scaffold has proven to be a challenging endeavor as beneficial modifications often compromise other functional properties. For example, phosphorothioate linkages that confer resistance to nuclease attack have been shown to reduce catalytic activity (Appaiahgari and Vrati, 2007). Similarly, modifications that increase the affinity of 10–23 for the RNA substrate can lead to product inhibition by stabilizing the enzyme-product complex formed after the phosphodiester bond cleavage step in the reaction pathway (Vester et al., 2002; Wang et al., 2021b). Recognizing the need for new chemotypes that enhance both in vivo stability and catalytic activity without sacrificing turnover, Wang and co-workers leveraged the unique physicochemical properties of different XNAs to develop a superior RNA-cleaving reagent based on the original 10–23 sequence (Wang et al., 2021b). The new catalyst, called X10-23, replaced all of the DNA residues in the substrate binding arms and two positions in the catalytic core with analogous FANA residues. To achieve enhanced biostability, TNA residues were added to the 5′ and 3′ termini to protect against nuclease degradation. The resulting XNAzyme achieved multiple turnover catalytic activity under simulated physiological conditions in vitro (1 mM $MgCl_2$ and pH 7.5), outcompeting previous state-of-the-art chemotypes, and showed persistent gene silencing in cultured mammalian cells by efficiently degrading targeted transcripts. However, as the known cellular toxicity of FANA could be problematic in therapeutic applications (McKenzie et al., 1995; Shen et al., 2018), X10-23 should be viewed as a model for how to improve the in vivo catalytic properties of 10–23.

6. XNAzyme applications

Rapid development of efficient XNAzymes has motivated research towards their potential use in a number of biomedical applications. In particular, the robust intracellular RNA cleavage capabilities of X10-23 make it an attractive candidate as a therapeutic gene silencing reagent (Fig. 3A). Unlike existing nucleic acid-based gene silencing technologies, such as antisense oligonucleotides (ASOs) and small interfering RNAs (siRNAs), X10-23 does not rely on cellular machinery (e.g., RNase H or the RISC complex), is refractory to nuclease digestion, and can distinguish target sequences that differ by a single nucleotide. Given its preference for cleavage at G-U junctions, X10-23 can perform allele-specific RNA knockdown in instances where a disease-associated point mutation creates a G-U dinucleotide in one or more copies of a specific gene. Nguyen et al. leveraged this feature of X10-23 to target one such mutation causing a deleterious glycine-to-valine substitution in the twelfth amino acid (G12V) of the Kirsten rat sarcoma viral oncogene homologue (KRAS) (Nguyen et al., 2021). In an adenocarcinoma cell line harboring both wild-type and G12V KRAS alleles, G12V-targeting X10-23 selectively reduced G12V transcripts by more than 50%, with minimal off-targeting of wild-type transcripts. This decrease in G12V expression ultimately reduced expression of phosphorylated MEK, a key downstream effector in the oncogenic KRAS signaling pathway. These results indicate that X10-23 may fill a niche in the pharmaceutical market for therapies targeting mutations like G12V in KRAS, which were previously considered “undruggable.”

Another clinically relevant application for XNAzymes is in nucleic acid detection for point-of-care diagnostic testing. Recently, a biosensing platform called REVEALR was designed by coupling isothermal amplification with a split X10-23 enzyme that cleaves a quenched RNA reporter to produce an optical signal in the presence of a viral RNA trigger (Yang and Chaput, 2021) (Fig. 3B). REVEALR achieved low attomolar-level sensitivity for SARS-CoV-2 detection in clinical patient-derived samples

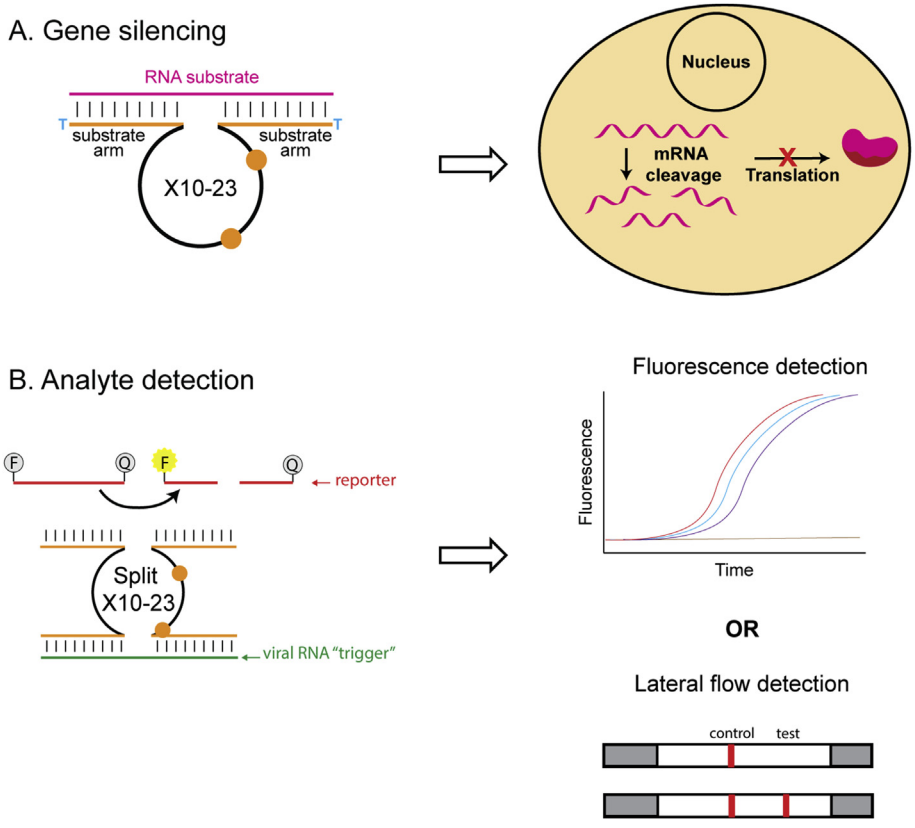

Fig. 3. XNAzyme applications. (A) A schematic of X10-23 is presented (*left*) with the catalytic core DNA sequence represented in black, FANA modifications in orange, and TNA modifications in blue. The RNA substrate is shown in pink. The application of X10-23 as an intracellular gene silencing reagent is schematized (*right*). (B) A schematic of Split X10-23 cleaving a fluorophore-quencher pair in the presence of a viral RNA trigger (*left*) is presented. The color scheme is the same as in (A). The fluorescence and paper-based outputs of the nucleic acid detection platform using Split X10-23 is schematized (*right*).

with no cross-reactivity observed for related respiratory viruses. Furthermore, the REVEALR-based assay can be implemented using a lateral-flow strip for facile testing and visual readout, making REVEALR a possible alternative to the CRISPR-Cas-based detection strategies, such as SHERLOCK (Gootenberg et al., 2017; Joung et al., 2020) and DETECTR (Chen et al., 2018; Broughton et al., 2020), for diagnosis of infectious diseases including COVID-19.

7. Conclusion

The unique chemical architectures of XNAzymes endow these molecules with key advantages over conventional nucleic acid-based technologies that may be exploited for diagnostic and therapeutic purposes. Current challenges in the field include the chemical synthesis of XNA triphosphates and oligonucleotides, the availability of XNA polymerases with higher fidelity and catalytic efficiency, and the unknown toxicity of many XNAs in cellular applications. Continued progress in these areas may lead to the development of XNAzymes with additional types or combinations of modified sugars, bases, or backbones, expanding the chemical properties of these reagents for more efficient and versatile catalysis against a broader range of targets.

Declaration of competing interest

The authors declare that they have no known competing financial interests or personal relationships that could have appeared to influence the work reported in this paper.

Acknowledgements

We would like to thank members of the Chaput laboratory for helpful discussions and critical reading of the manuscript. This work was supported by a grant from the W.M. Keck Foundation and by grants from the National Science Foundation [CHE: 2001434 and MCB: 1946312].

References

Anosova, I., Kowal, E.A., Dunn, M.R., Chaput, J.C., Van Horn, W.D., Egli, M., 2016. The structural diversity of artificial genetic polymers. Nucleic Acids Res. 44, 1007–1021.
Appaiahgari, M.B., Vrati, S., 2007. DNAzyme-mediated inhibition of Japanese encephalitis virus replication in mouse brain. Mol. Ther. 15, 1593–1599.
Breaker, R.R., Joyce, G.F., 1994. A DNA enzyme that cleaves RNA. Chem. Biol. 1, 223–229.
Broughton, J.P., Deng, X., Yu, G., Fasching, C.L., Servellita, V., Singh, J., Miao, X., Streithorst, J.A., Granados, A., Sotomayor-Gonzalez, A., et al., 2020. CRISPR-Cas12-based detection of SARS-CoV-2. Nat. Biotechnol. 38, 870–874.
Brudno, Y., Liu, D.R., 2009. Recent progress toward the templated synthesis and directed evolution of sequence-defined synthetic polymers. Chem. Biol. 16, 265–276.
Cech, T.R., Zaug, A.J., Grabowski, P.J., 1981. In vitro splicing of the ribosomal RNA precursor of Tetrahymena: involvement of a guanosine nucleotide in the excision of the intervening sequence. Cell 27, 487–496.
Chaput, J.C., Herdewijn, P., 2019. What is XNA? Angew Chem. Int. Ed. Engl. 58, 11570–11572.
Chen, J.S., Ma, E., Harrington, L.B., Da Costa, M., Tian, X., Palefsky, J.M., Doudna, J.A., 2018. CRISPR-Cas12a target binding unleashes indiscriminate single-stranded DNase activity. Science 360, 436–439.
Cho, E.A., Moloney, F.J., Cai, H., Au-Yeung, A., China, C., Scolyer, R.A., Yosufi, B., Raftery, M.J., Deng, J.Z., Morton, S.W., et al., 2013. Safety and tolerability of an intratumorally injected DNAzyme, Dz13, in patients with nodular basal-cell carcinoma: a phase 1 first-in-human trial (DISCOVER). Lancet 381, 1835–1843.
Cochrane, W.G., Malone, M.L., Dang, V.Q., Cavett, V., Satz, A.L., Paegel, B.M., 2019. Activity-based DNA-encoded library screening. ACS Comb. Sci. 21, 425–435.
Colville, B.W.F., Powner, M.W., 2021. Selective prebiotic synthesis of alpha-threofuranosyl cytidine by photochemical anomerization. Angew Chem. Int. Ed. Engl. 60, 10526–10530.
Culbertson, M.C., Temburnikar, K.W., Sau, S.P., Liao, J.Y., Bala, S., Chaput, J.C., 2016. Evaluating TNA stability under simulated physiological conditions. Bioorg. Med. Chem. Lett. 26, 2418–2421.
Dunn, M.R., McCloskey, C.M., Buckley, P., Rhea, K., Chaput, J.C., 2020. Generating biologically stable TNA aptamers that function with high affinity and thermal stability. J. Am. Chem. Soc. 142, 7721–7724.
Ekland, E.H., Bartel, D.P., 1996. RNA-catalysed RNA polymerization using nucleoside triphosphates. Nature 382, 373–376.
Ekland, E.H., Szostak, J.W., Bartel, D.P., 1995. Structurally complex and highly active RNA ligases derived from random RNA sequences. Science 269, 364–370.
Fitzgerald, P.R., Paegel, B.M., 2021. DNA-encoded chemistry: drug discovery from a few good reactions. Chem. Rev. 121, 7155–7177.
Gootenberg, J.S., Abudayyeh, O.O., Lee, J.W., Essletzbichler, P., Dy, A.J., Joung, J., Verdine, V., Donghia, N., Daringer, N.M., Freije, C.A., et al., 2017. Nucleic acid detection with CRISPR-Cas13a/C2c2. Science 356, 438–442.
Goto, Y., Katoh, T., Suga, H., 2011. Flexizymes for genetic code reprogramming. Nat. Protoc. 6, 779–790.
Guerrier-Takada, C., Gardiner, K., Marsh, T., Pace, N., Altman, S., 1983. The RNA moiety of ribonuclease P is the catalytic subunit of the enzyme. Cell 35, 849–857.
Hollenstein, M., 2019. Nucleic acid enzymes based on functionalized nucleosides. Curr. Opin. Chem. Biol. 52, 93–101.
Joung, J., Ladha, A., Saito, M., Kim, N.G., Woolley, A.E., Segel, M., Barretto, R.P.J., Ranu, A., Macrae, R.K., Faure, G., Ioannidi, E.I., Krajeski, R.N., Bruneau, R., Huang, M.W., Yu, X.G., Li, J.Z., Walker, B.D., Hung, D.T., Greninger, A.L., Jerome, K.R., Gootenberg, J.S., Abudayyeh, O.O., Zhang, F., 2020. Detection of SARS-CoV-2 with SHERLOCK one-pot testing. N. Engl. J. Med. 383, 1492–1494.
Joyce, G.F., 2004. Directed evolution of nucleic acid enzymes. Annu. Rev. Biochem. 73, 791–836.
Kauppinen, S., Vester, B., Wengel, J., 2005. Locked nucleic acid (LNA): high affinity targeting of RNA for diagnostics and therapeutics. Drug Discov. Today Technol. 2, 287–290.
Kim, H.J., Benner, S.A., 2017. Prebiotic stereoselective synthesis of purine and noncanonical pyrimidine nucleotide from nucleobases and phosphorylated carbohydrates. Proc. Natl. Acad. Sci. U. S. A. 114, 11315–11320.
Kratschmer, C., Levy, M., 2017. Effect of chemical modifications on aptamer stability in serum. Nucleic Acid Ther. 27, 335–344.
Lohse, P.A., Szostak, J.W., 1996. Ribozyme-catalysed amino-acid transfer reactions. Nature 381, 442–444.
McKenzie, R., Fried, M.W., Sallie, R., Conjeevaram, H., Di Bisceglie, A.M., Park, Y., Savarese, B., Kleiner, D., Tsokos, M., Luciano, C., et al., 1995. Hepatic failure and lactic acidosis due to fialuridine (FIAU), an investigational nucleoside analogue for chronic hepatitis B. N. Engl. J. Med. 333, 1099–1105.
Nguyen, K., Wang, Y., England, W.E., Chaput, J.C., Spitale, R.C., 2021. Allele-specific RNA knockdown with a biologically stable and catalytically efficient XNAzyme. J. Am. Chem. Soc. 143, 4519–4523.
Nikoomanzar, A., Chim, N., Yik, E.J., Chaput, J.C., 2020. Engineering polymerases for applications in synthetic biology. Q. Rev. Biophys. 53, e8.
Nissen, P., Hansen, J., Ban, N., Moore, P.B., Steitz, T.A., 2000. The structural basis of ribosome activity in peptide bond synthesis. Science 289, 920–930.
Pinheiro, V.B., Taylor, A.I., Cozens, C., Abramov, M., Renders, M., Zhang, S., Chaput, J.C., Wengel, J., Peak-Chew, S.Y., McLaughlin, S.H., et al., 2012. Synthetic genetic polymers capable of heredity and evolution. Science 336, 341–344.
Pinheiro, V.B., Loakes, D., Holliger, P., 2013. Synthetic polymers and their potential as genetic materials. Bioessays 35, 113–122.
Prody, G.A., Bakos, J.T., Buzayan, J.M., Schneider, I.R., Bruening, G., 1986. Autolytic processing of dimeric plant virus satellite RNA. Science 231, 1577–1580.
Santoro, S.W., Joyce, G.F., 1997. A general purpose RNA-cleaving DNA enzyme. Proc. Natl. Acad. Sci. U. S. A. 94, 4262–4266.
Santoro, S.W., Joyce, G.F., 1998. Mechanism and utility of an RNA-cleaving DNA enzyme. Biochemistry 37, 13330–13342.
Schmidt, M., 2010. Xenobiology: a new form of life as the ultimate biosafety tool. Bioessays 32, 322–331.
Shen, W., De Hoyos, C.L., Sun, H., Vickers, T.A., Liang, X.H., Crooke, S.T., 2018. Acute hepatotoxicity of 2' fluoro-modified 5-10-5 gapmer phosphorothioate oligonucleotides in mice correlates with intracellular protein binding and the loss of DBHS proteins. Nucleic Acids Res. 46, 2204–2217.
Silverman, S.K., 2008. Nucleic acid enzymes (Ribozymes and Deoxyribozymes): in vitro selection and application. In: Begley, T.P. (Ed.), In Wiley Encyclopedia of Chemical Biology, 10.1002/9780470048672.wecb406.
Smuga, D., Majchrzak, K., Sochacka, E., Nawrot, B., 2010. RNA-cleaving 10–23 deoxyribozyme with a single amino acid-like functionality operates without metal ion cofactors. New J. Chem. 34, 934.
Tarasow, T.M., Tarasow, S.L., Eaton, B.E., 1997. RNA-catalysed carbon-carbon bond formation. Nature 389, 54–57.
Taylor, A.I., Pinheiro, V.B., Smola, M.J., Morgunov, A.S., Peak-Chew, S., Cozens, C., Weeks, K.M., Herdewijn, P., Holliger, P., 2015. Catalysts from synthetic genetic polymers. Nature 518, 427–430.
Tjhung, K.F., Shokhirev, M.N., Horning, D.P., Joyce, G.F., 2020. An RNA polymerase ribozyme that synthesizes its own ancestor. Proc. Natl. Acad. Sci. U. S. A. 117, 2906–2913.
Unrau, P.J., Bartel, D.P., 1998. RNA-catalysed nucleotide synthesis. Nature 395, 260–263.
Vester, B., Lundberg, L.B., Sorensen, M.D., Babu, B.R., Douthwaite, S., Wengel, J., 2002. LNAzymes: incorporation of LNA-type monomers into DNAzymes markedly increases RNA cleavage. J. Am. Chem. Soc. 124, 13682–13683.
Wang, Y., Ngor, A.K., Nikoomanzar, A., Chaput, J.C., 2018. Evolution of a general RNA-cleaving FANA enzyme. Nat. Commun. 9, 5067.
Wang, Y., Vorperian, A., Shehabat, M., Chaput, J.C., 2020. Evaluating the catalytic potential of a general RNA-cleaving FANA enzyme. Chembiochem 21, 1001–1006.
Wang, Y., Wang, Y., Song, D., Sun, X., Zhang, Z., Li, X., Li, Z., Yu, H., 2021. A threose nucleic acid enzyme with RNA ligase activity. J. Am. Chem. Soc. 143, 8154–8163.
Wang, Y., Nguyen, K., Spitale, R.C., Chaput, J.C., 2021. A biologically stable DNAzyme that efficiently silences gene expression in cells. Nat. Chem. 13, 319–326.
Wilson, C., Szostak, J.W., 1995. In vitro evolution of a self-alkylating ribozyme. Nature 374, 777–782.

Wilson, D.S., Szostak, J.W., 1999. In vitro selection of functional nucleic acids. Annu. Rev. Biochem. 68, 611–647.
Wu, H.N., Lin, Y.J., Lin, F.P., Makino, S., Chang, M.F., Lai, M.M., 1989. Human hepatitis delta virus RNA subfragments contain an autocleavage activity. Proc. Natl. Acad. Sci. U. S. A. 86, 1831–1835.
Xie, Y.Y., Zhao, X.D., Jiang, L.P., Liu, H.L., Wang, L.J., Fang, P., Shen, K.L., Xie, Z.D., Wu, Y.P., Yang, X.Q., 2006. Inhibition of respiratory syncytial virus in cultured cells by nucleocapsid gene targeted deoxyribozyme (DNAzyme). Antivir. Res. 71, 31–41.
Yang, K., Chaput, J.C., 2021. REVEALR: a multicomponent XNAzyme-based nucleic acid detection system for SARS-CoV-2. J. Am. Chem. Soc. 143, 8957–8961.
Yang, K., McCloskey, C.M., Chaput, J.C., 2020. Reading and writing digital information in TNA. ACS Synth. Biol. 9, 2936–2942.
Yu, H., Zhang, S., Chaput, J.C., 2012. Darwinian evolution of an alternative genetic system provides support for TNA as an RNA progenitor. Nat. Chem. 4, 183–187.
Zhang, B., Cech, T.R., 1997. Peptide bond formation by in vitro selected ribozymes. Nature 390, 96–100.